Electrified Hydraulic Power Steering System in Hybrid Electric Heavy Trucks

C. Morton* , C. M. Spargo* & V. Pickert

*School of Electrical and Electronic Engineering, Merz Court, University of Newcastle Upon Tyne, UK

Abstract

Over the last 20 years conventional automotive engine ancillaries have migrated from being mechanically powered to electrically powered in order to meet market demand. To adopt this trend in heavy trucks requires a higher power electrical system in order to cope with the higher loads placed upon it. Until the advent of the Hybrid Electric heavy Truck (HET) this power infrastructure has not been available. HET's require a higher voltage system in order to reduce losses and provide adequate power and voltage levels for the traction motor. This paper investigates for the first time the benefit of electrifying a Hydraulic Power assisted Steering (HPS) system in an HET. The developed Electrical Hydraulic Power Steering (EHPS), using a high voltage traction battery, is found to drastically reduce the consumed energy over a drive cycle by optimal operation of the pump over the driving cycle. Empirical data from a prototype HET with EHPS confirms the simulation results from Dymola.

1. Introduction

Power assisted steering systems are essential in truck applications as it assists drivers to steer the truck with only modest efforts. All truck steering systems have a mechanical connection between steering wheel and the linkage that steers the road wheels [1-3]. These systems are hydraulically powered with the hydraulic pressure being supplied either from an engine-driven pump (using a belt and pulley arrangement) or connected directly to the crankshaft. These systems are referred to as Hydraulic Power assisted Steering (HPS) systems. In conventional engine driven configurations the hydraulic pump is mechanically driven by the engine as shown in Fig. 1.

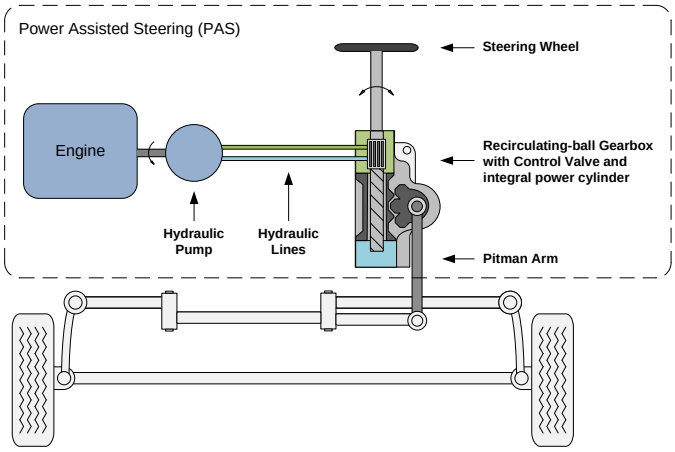

Fig. 1. Generalised HPS steering layout

The direct mechanical coupling forces the pump speed to be directly governed by the engine speed. This severely limits the ability to control its operating conditions and hence the efficiency of the pump [4] over the drive cycle.

The vehicle's weight and suspension geometry determine the magnitude of steering force required to manoeuvre the wheels. This determines the size of the hydraulic pump required for the vehicle. The fluid pressure and flow at low engine speeds are proportional to the required torque and power required to drive the pump and this is usually chosen as the pump design criteria. This is because the greatest demand for steering assistance is at low speed during slow speed manoeuvres [5].

As the engine speeds up (and hydraulic pressure increases), the pump's internal pressure relief valve opens in order to limit fluid pressure within the system (t=902s in Fig. 2); the pump's torque remains approximately constant, but the consumed power tracks and increases almost linearly with engine speed, as shown in Fig. 2.

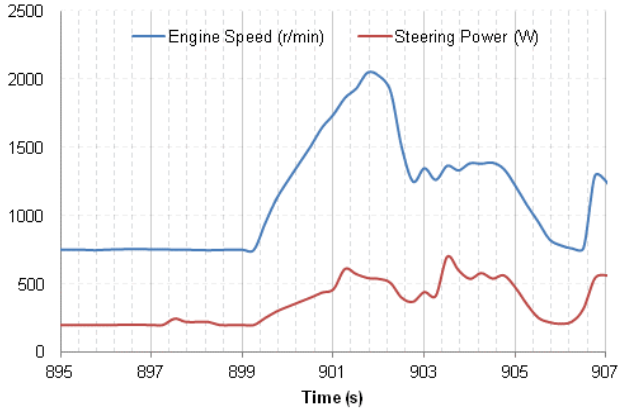

Fig. 2. Example of power consumption profile of a mechanically driven power steering pump

Additionally, even when the pump is unloaded, internal mechanical friction losses and viscous friction losses caused by circulating fluid which is not performing work on the steering column will cause small, but non-negligible power consumption.

If the hydraulic pump is decoupled from the engine and driven by an electric motor, it can be operated independently from the engine. This system is commonly referred to as an Electrical Hydraulic Power Steering system (EHPS), as shown in Fig. 3. As the speed of the pump is not coupled to the engine speed it can be driven only when required and then at the highest efficiency operating point. This has the effect of reducing the power demand of the system dramatically, while maintaining all the benefits of a hydraulic system, such as 'road feel' [6].

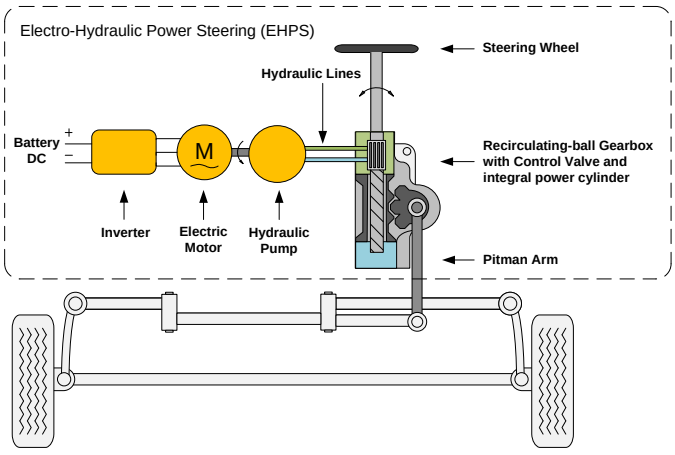

Fig. 3. Generalised EHPS steering layout

The principal reason the truck industry has not embraced this technology sooner is due to the limits of a conventional truck's electrical system. Conventional trucks have been using a standardised 24 V_{DC} electrical bus since the mid 1960's. This low voltage system is more than adequate to handle the demands of cab electrical devices in conventional trucks. However, when the vehicle's engine ancillaries (water pump, air conditioning compressor, power steering, etc.) are to be electrified, the 24 V_{DC} bus is unable to cope with the power demands placed upon it. An attempt to draw higher power from the 24 V_{DC} bus would result in substantial power loss from heat dissipation in the ancillaries' cabling.

For example if electrifying an HPS system in a heavy truck with a 24 V_{DC} system, where typical peak power requirements of up to 5 kW are seen for worse case steering manoeuvres, currents of over 200 Amps on the 24 V_{DC} bus would be demanded, generating enormous losses not only in cables but also in the battery.

Heavy-weight trucks omit the use of EHPS because the common 24 V truck battery cannot provide the power that is necessary to drive an electrically driven power steering pump. Hybrid Electric Trucks (HET), however, have a second high voltage battery as part of their power drive train capable of providing sufficient power to drive the EHPS. An ancillary electric motor powered from the high voltage traction battery, coupled to a hydraulic power steering pump could be operated at maximum efficiency throughout the drive cycle, reducing energy consumption.

2. Data gathering

In order to evaluate current limitations of a standard truck's HPS system, it is necessary to retrieve data from the standard truck's HPS system. A local test route was developed by a major truck manufacturer to simulate a typical route used by major retail chains in the inner-city. The route is shown in Fig. 4a.

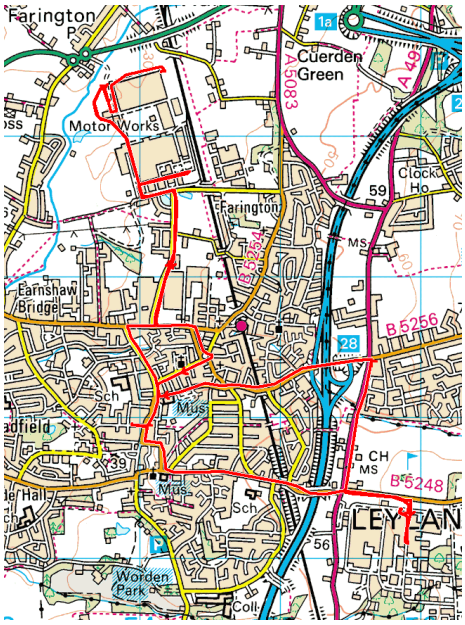

a.

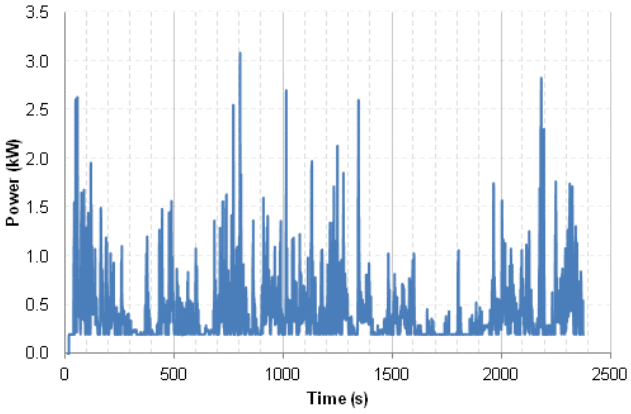

b.

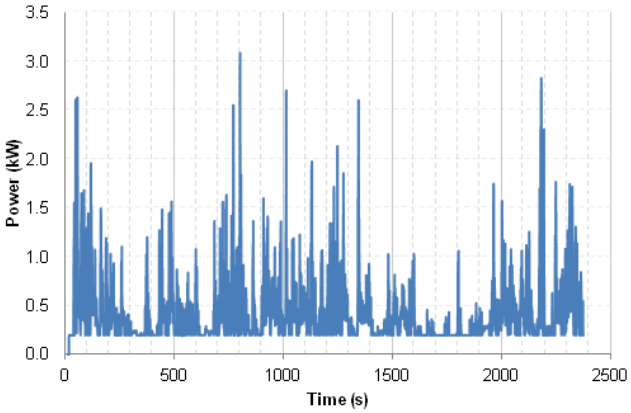

c.

Fig. 4. Test route recorded results for FR1
a. Steering drive cycle (in red) for the collection of data for the HPS system.
b. HPS steering power over the test route FR1 (The cycles have a maximum peak power of 3.1 kW at 795s.)
c. HPS pump torque over test route FR1. (Maximum peak shaft torque of 36.8 N·m at 2259 s)

A 12 ton HET truck (parallel hybrid) was wired with data acquisition equipment in order to measure the vehicle's parameters. The real-time telemetry data provided the ability to log system parameters over CAN bus in real time, such as the power steering pump pressure, engine speed, vehicle speed and GPS data. The route was mainly covering the village of Farington in the UK and is defined as test route FR1. From these measurements two of the most important HPS characteristics can be calculated: mechanical power on the shaft (P_{shaft}) and torque (T_{shaft}) (acting between the steering column and pump). Which can be calculated from the engine speed ω, pump pressure p and flow q. Eq. (1) shows the relationship between mechanical power P_{shaft}, the engine speed ω (r/min), pump pressure p and flow q. Eq. (2) shows the relationship between torque T_{shaft}, engine speed ω (in r/min), and mechanical power P_{shaft} (in r/min),.

$$P_{shaft} = \frac{q\ P}{1714\ E} \tag{1}$$

$$\tau_{shaft} = \frac{63025 P_{shaft}}{\omega} \tag{2}$$

Fig. 4b, 4c show the recorded steering power and pump torque results for FR1 steering drive cycle.

Although test route FR1 represents a typical truck driving cycle, the cycle does not reflect the worst-case steering manoeuvre. This is commonly known as the dry park manoeuvre, which is considered to be the most severe power demanding steering input [7]. The test was performed at standstill with the vehicle brakes applied in order to induce as much tyre scrub as possible. At dry park, peak torque is 44N.m at 798rpm resulting in a peak power of 4.5kW this would translate to a electric motor volume of approximately 7500 cm^3 which was deemed too large by the collaborating truck manufacturer.
In order to reduce the maximum peak torque in order to decrease motor size, it was decided to redesign the current steering pump. This was performed by the existing pump's manufacturer, who increased the speed of the pump to 1800 r/min and reduced the volumetric capacity, thus reducing the shaft torque while maintaining the required power level. Eq. (3) shows the relation between mechanical shaft power P_{shaft}, torque T_{shaft} and speed ω_{shaft}.

$$P_{shaft} = \tau_{shaft}\ \omega_{shaft} \tag{3}$$

The higher pump speed reduces the torque to 18 N·m. In sizing an electrical machine, for a given torque specification, the rotor volume V_r is related to the developed electromagnetic power P_{em} by the following relation Eq. (4);

$$P_{em} = \omega_{shaft} 2\sigma_{Ftan} V_r \tag{4}$$

Where σ_{Ftan}, is the tangential Maxwell shear stress on the rotor surface Eq. (5). For as open circuit cooled permanent magnet machine;

$$\sigma_{Ftan} = 33500 \cos(\varphi) \tag{5}$$

The power factor $\cos(\varphi)$ is assumed as 0.9, thus the tangential stress dictates the required rotor volume for a given torque, equal to 30.485 kPa. Assuming the same tangential stress in both machines, the following ratio can be defined Eq. (6);

$$\frac{P_{em1}}{P_{em2}} = 1 = \frac{798\,V_{r1}}{1800 V_{r2}} \quad (6)$$

Solving for V_{r2} the rotor volume is required to be around 0.45 times that of the original rotor volume, with the total machine volume following suit. Selecting a motor to meet the new pump specification for a maximum peak torque of 18 N·m substantially reduces the size of the motor to approximately 3700 cm^3.

3. Simulations

To simulate the EHPS system, a model was designed using Dymola® Vehicle Dynamics Library (VDL) truck components. Dymola® VDL is commonly used throughout the automotive industry for simulating vehicle systems. The model design parameters are based on a 12 ton HET truck as shown in Fig. 5. The dimensions used in the model were taken from the actual vehicle and are listed in Table 1.

Fig. 5. HET experimental vehicle

Table.1. Simulation system parameters

Model parameters		
	Value	**Unit**
EHPS		
Maximum battery voltage	403	V
Nominal battery voltage	340	V
Minimum battery voltage	270	V
Maximum motor current	34	A
Torque current ratio	1.65	N·m/A
Motor inertia	13.548	Kg-cm^2
Stator Resistance	0.92	Ohm
Max. motor speed	2250	rpm
Peak pump power	3.8	kW
Peak pump torque	18	N·m
Nominal pump shaft speed	1800	r/min
Nominal Battery voltage	340	VDC
Battery capacity	14.1	kWh
EHPS motor type	BLDC, 3Ph, 8Pole, 340V	
EHPS controller type	3 Phase, 6 Step commutation	
Battery type	A123 (Nanophosphate)	
Vehicle		
Steering gear	Integrated recirculating ball gearbox	

	with pitman arm
Front Suspension	Standard Steel Parabolic
Steering gear ratio	20:1

3.1 Dymola Model

The control scheme chosen for the EHPS inverter is a closed loop constant speed control system, shown in Fig. 6. This consists of two feedback loops, a fast inner control loop that is used to regulate output current and a slower outer speed control loop used to maintain motor speed. This nested two loop structure is commonly used in motor drive control applications due to the ease of implementation, favourable control characteristics and from an equipment protection point of view [8, 9].

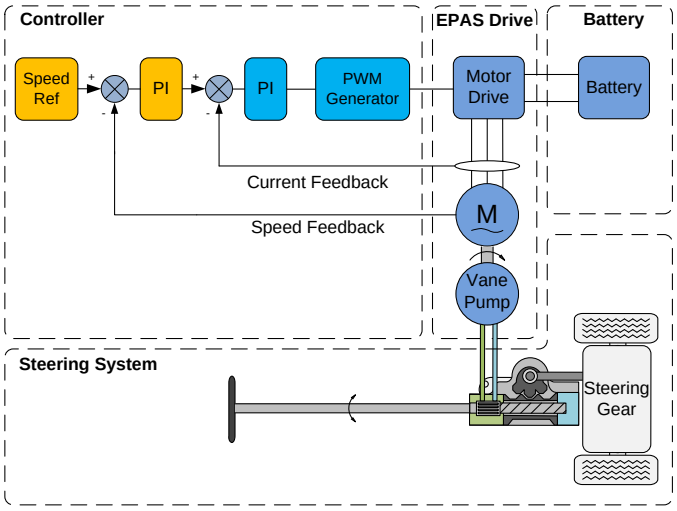

Fig. 6. Model of the EHPS Controller

Fig. 6 also shows the complete EHPS system in context, from battery to steering pump. The battery is a 14.1 kWh Nanophosphate type, that has a working voltage range of 270 V_{DC} to 403 V_{DC}. The battery is connected to the drive's power electronics sub-system that comprises of the DC link capacitor and Insulated Gate Bipolar Transistor (IGBT) 3 phase module. The output of the power electronics sub-system feeds in to a BLDC motor where the output shaft feeds into the measured torque load profiles of the hydraulic steering pump shown in Fig. 6.

Three battery and two pump load conditions have been simulated in this model. Simulations were run at the minimum and maximum battery voltages of 270 V_{DC} and 403 V_{DC} respectively as well as at the nominal voltage of 340 V_{DC}. A fixed maximum pump load of 18 N·m and worst case battery voltage was used to determine maximum current and power of the EHPS. Finally a torque step response was applied to test the dynamic response of the system.

3.2 Simulation Results

In order to analyse the energy benefits of the EHPS system a series of test manoeuvres were simulated in the Dymola® model to gain an understanding of the behaviour of the system.

3.2.1 Worst case EHPS motor currents at maximum load

The simulated inverter input current waveform is shown in Fig. 7a measured between the vehicle battery and the inverter. The waveform was simulated with the maximum pump load of 18 N·m applied, as specified by the pump manufacturer and the worst case battery voltage

of 270 V_{DC} as specified by the electrical system manufacturer. The maximum simulated mean current draw of the inverter was calculated as 12.7 A.

The simulated inverter's output current waveform is shown in Fig. 7b measured between the inverter and BLDC motor. The waveform was simulated with the maximum pump load of 18 N·m and the worst case battery voltage of 270 V_{DC}. The maximum simulated RMS current draw of the inverter was calculated to 12.8 A.

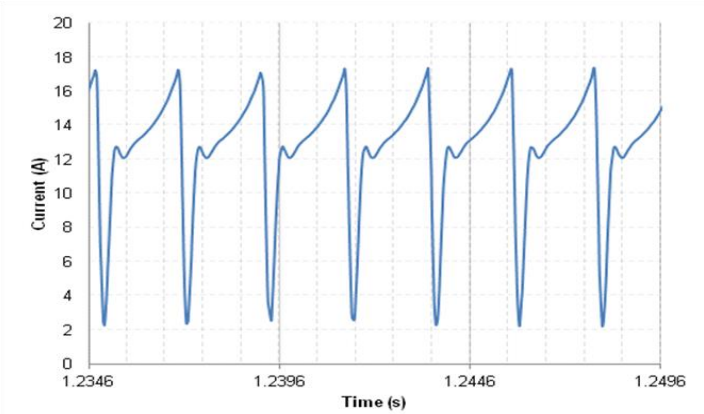

a.

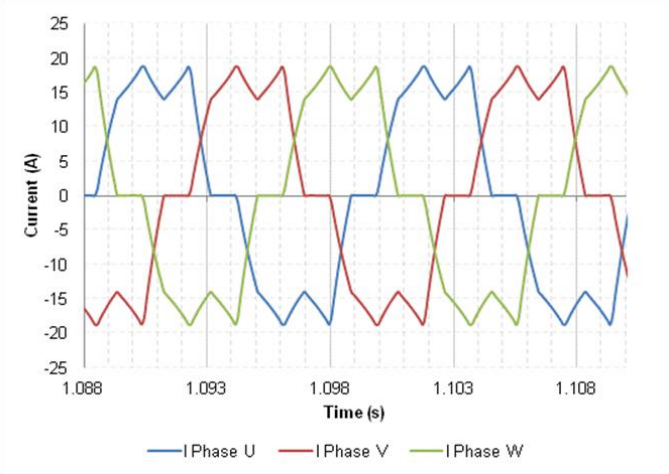

b.

Fig. 7. Worst case simulated EHPS currents

a. Worst case simulated inverter input current at 18 N·m static load condition.
b. Worst case simulated inverter output currents at 18 N·m static load condition.

3.2.2 Simulated EHPS motor speed response

The motor's speed response to a change in load is shown in Fig. 8. At 0.6s, from 1.03 N·m to 18 N·m. With supply voltages of 403 and 340 V_{DC} the speed returns to the required set point of 1800 r/min, However when the supply voltage falls to 270 V_{DC} it can be seen the motor speed drops to 1440 r/min. The reason for the failure to return to the speed set point is due to the motor's back EMF characteristic since as the supply voltage reduces, the difference between the motor's back EMF and the applied motor voltage is reduced.

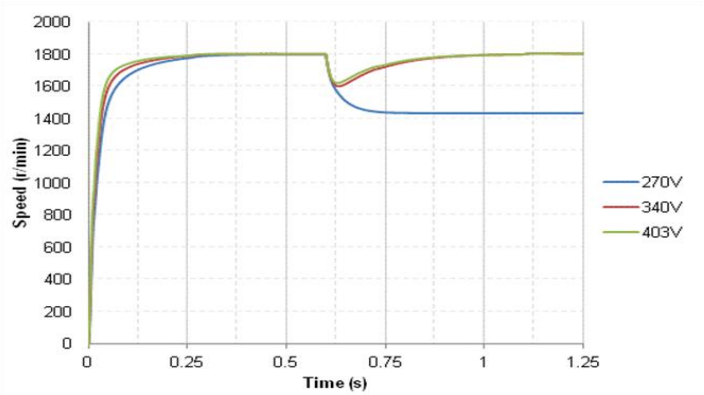

Fig. 8. Simulated motor speed response to a change in load

This leads to the condition where not enough current can be induced in the motor at the given torque load, hence the speed is reduced. This effect can be analytically described in Eq. (7).

$$V = iR + L\frac{di}{dt} + E \tag{7}$$

Where E is the back EMF induced in the armature windings by the magnetic field. I is the phase current, R the resistance of the motor windings per phase and L is the phase inductance. Eq. (7) shows that a rise in E must result in a drop of I at constant V.

3.2.3 HPS vs. simulated EHPS power consumption comparison

A comparison between the current HPS system and the simulated output of the proposed EHPS system is shown in Fig. 9 using the dynamic pump load data from the FR1 test route shown in Fig. 4a.

The initial simulation results for the test route FR1 indicate the overall energy consumption of the EHPS is less than the consumption of the HPS. The total recorded HPS energy consumption is 2914.2 kJ while the simulated EHPS energy consumption is 971.3 kJ. This is an energy reduction of more than 66% and this makes the EHPS system very attractive for truck applications.

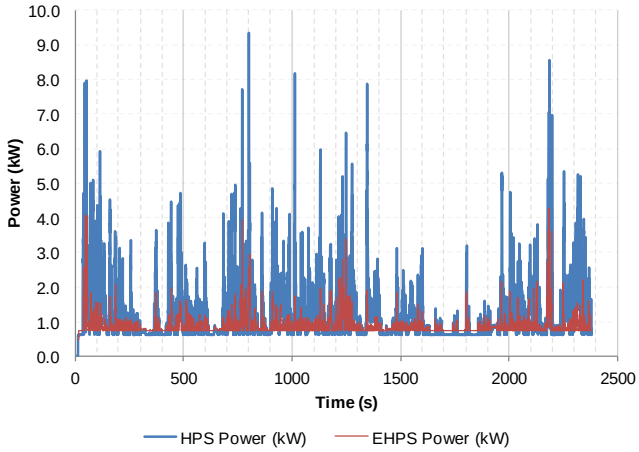

Fig. 9. Actual HPS vs. simulated EHPS power consumption comparison

The overall simulated electrical efficiency for the drive has been calculated for test route FR1 using Eq. (8)

$$\eta = \frac{Energy\ Out\ (kJ)}{Energy\ In\ (kJ)} \quad (8)$$

Hence for test route FR1 the total calculated efficiency for the simulated EHPS is 74.5% and the efficiency of the HPS is 33.0%.

4. Hardware Implementation

4.1 Controller hardware

The controller is based on a Microchip 30F2023 DsPic MCU (Micro Controller Unit). This is a 16 bit fixed point microcontroller operating at 40 MHz. A custom control PCB was designed to accommodate the MCU, signal filtering and multilevel power supplies needed for the control of the inverter.

The constants for the proportional and integral gains *Kp* and *Ki* for each loop were obtained by the 2nd method formula table proposed by Ziegler and Nichols [10, 11] and the final control parameters are presented in Table 2.

Table. 2. *Kp* and *Ki* values

Gain	Position Loop	Speed Loop	Current Loop
Kp	0.2	0.2	0.5
Ki		0.02	0.08

As the inner current loop needs to respond to fast changes in current, the sampling time Δt for the inner loop has been derived directly from the DsPic PWM timer and is set at 100 μs, with the speed loop is sampled at 500 μs. The position loop of a control scheme is sampled at 1ms as it is not necessary for such a fast sample period due to the relatively slow change in pump speed.

4.2 EHPS Test setup

The test rig for the EHPS power steering project is shown in Fig. 10a. The EHPS BLDC motor is coupled to a Permanent Magnet Synchronous Machine PMSM motor via a torque transducer. The torque transducer used is a 50 N·m torque meter with accuracy of 0.18%. A commercial industrial drive was used to control the PMSM load motor in order to emulate the steering pump torque profiles. The drive was programmed in such a way that it reproduced the actual pump torque from the steering test cycle and worst case dry park manoeuvre.

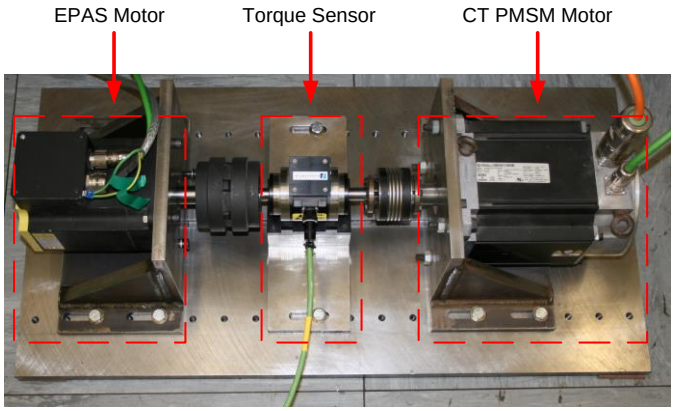

a.

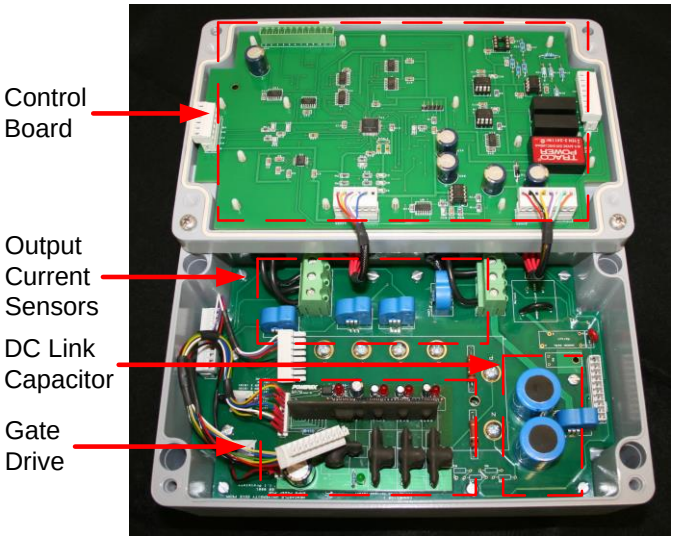

b.

Fig. 10. EHPS steering test rig bed plate and EHPS inverter
a. EHPS Dynamometer test bed showing EHPS Motor and PMSM load motor
b. EHPS Inverter

4.3 EHPS inverter

The inverter comprises of three symmetrical half bridges using IGBT's with freewheel diodes integrated in a common package module manufactured by PowerEX (PM75RLA060_E). This IGBT module is supplied by the DC input via a 100 μF low ESR electrolytic DC Link capacitor. The output of each phase was taken from the midpoint of each half bridge via Hall-effect current sensors. The output feeders then connect directly to the BLDC motor.

The gate drive PCB shown in Fig. 10b is based on the PowerEX VLA606-01R opto-interface IC and the VLA106-24154 isolated DC/DC converters. These are used to provide isolation of the control signals and isolated power for the built-in gate drive and protection circuits. A custom power PCB was designed to incorporate all the power electronic components.

5. Experimental Results

The EHPS system was tested using the test setup shown in Fig. 10a. The results not only provide a comparison with the truck's standard HPS system but in addition provide verification of the EHPS simulations.

Fig. 11a shows the inverter's input current waveform measured between the DC power supply and the inverter. The waveform was measured with the maximum pump load of 18 N·m and the worst case battery voltage of 270 V_{DC}. The maximum measured mean current draw of the inverter was 12.3 A.

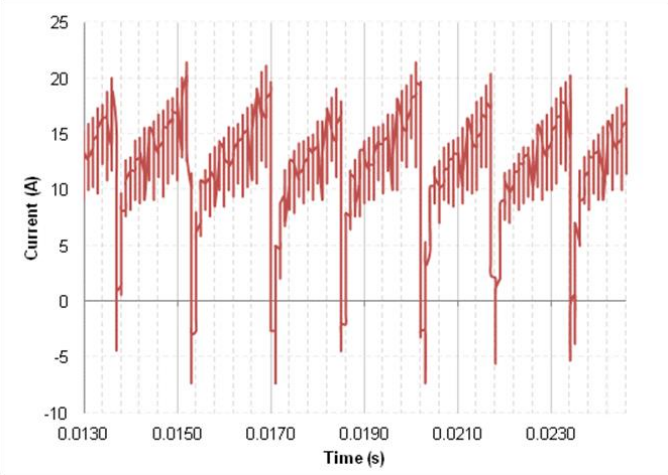

a.

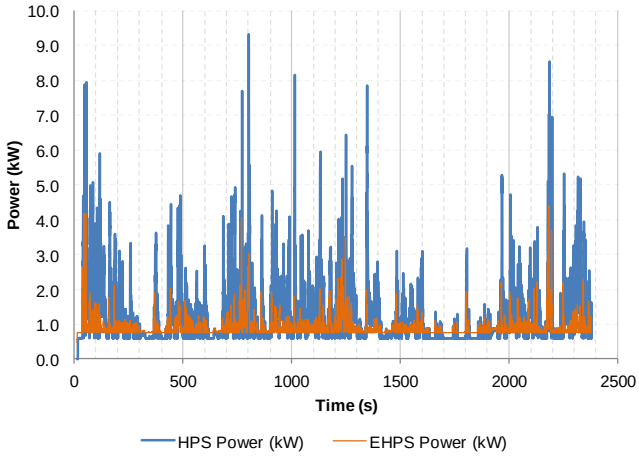

b.

Fig. 11. Worst case measured EHPS inverter
a. Worst case measured EHPS inverter input current at 18 N·m static load condition.
b. Actual HPS vs. Measured EHPS power consumption comparison

Fig. 11b shows the power consumption of the current HPS and EHPS systems using the dynamic pump load data from the FR1 test route. The test was carried out using the nominal system battery voltage of 340 Volts deemed to be the average working voltage of the battery by the electrical system manufacturer. The energy consumption of the EHPS system over the full duration of the test run was calculated at 1005.6 kJ making it 65.3% more efficient than the current HPS system for the FR1 test route.

6. Practical Considerations

It must be mentioned at this stage that although there are obvious benefits in energy savings associated with implementing an EHPS on a truck, in reality there are numerous reasons for this type of system having had a slow uptake in implementation on heavy vehicles.

When retro fitting an EHPS system to a conventional truck it was noted that there is no ideal placement. Due to the location of existing sub-systems most of the available spaces in which to package the EHPS were a compromise for the following reasons; (i) The available space subjected the EHPS to adverse mechanical and environmental conditions as shown in Fig. 12a, (ii) the location was sufficiently distant from the steering gear such that the increase in length of the high pressure hydraulic fluid lines would adversely affect the flow and pressure requirements.

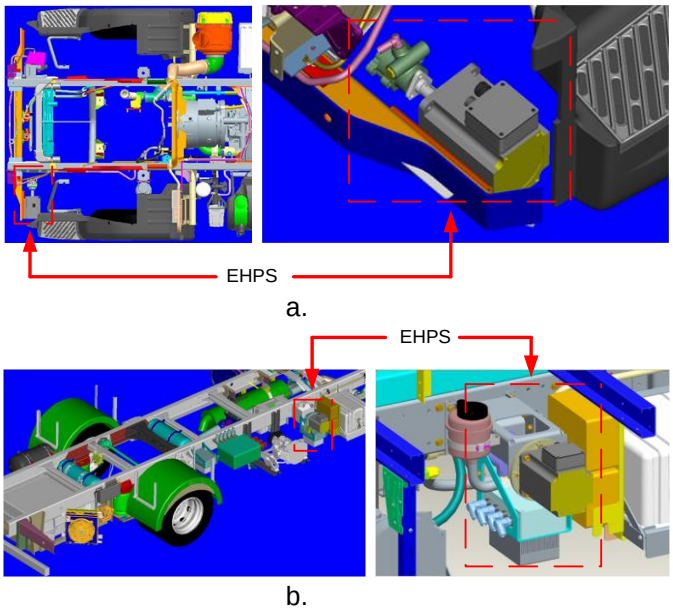

Fig. 12. Packaging locations for EHPS
a. Ideal location of EHPS fitted to front bumper under run cross member
b. Final location of EHPS fitted to chassis frame

It was therefore decided to place the EHPS on the chassis frame as shown in Fig. 12b. This location, although not ideal reduced the power cabling and hydraulic feed lengths to acceptable limits as well as placing the inverter in favourable environmental conditions.

This packaging exercise shows that the statement “EHPS reduces packaging problems” should be chosen carefully when publishing.

The final discussion point is the additional cost of the inverter and motor used in the EHPS system. The basic component costs at the time of writing are given in Table 3 [12] illustrating how the additional components used in the EHPS system substantially increase the price compared to the HPS.

Table. 3. Cost comparison of HPS and EHPS systems

Component costing		
	HPS	**EHPS**
Pump	£450	£450
Steering gear	£800	£800

Inverter		£220
Motor		£350
Total	£1250	£1820

In order to justify the extra cost of an EHPS system the fuel savings of the hybrid electric truck fitted with an EHPS system and HPS system are compared. The mile per gallon equivalent is calculated using Eq. (10).

$$MPGe = \frac{E_G}{E_M \times E_E} \tag{9}$$

Where, MPGe is expressed as miles per gallon equivalent, E_G is the energy content per gallon of diesel. E_G is equal to 37.95 (kWh) as set by United States Department of Energy (U.S. DoE) and reported by the Alternative Fuel Data Centre (AFDC) [13], E_M is the battery-to-wheel electrical energy consumed per mile (kWh/mi) plus the diesel energy consumed as measured over the FR1 test route [14], E_E is the energy per kW/h of electricity (J/Wh) equal to 3.412 [13].

MPGe values for the hybrid truck were calculated for the HPS and EHPS steering systems with data recorded form the FR1 test route. The MPGe were calculated at 11.83 MPGe for the HPS and 11.89 MPGe for the EHPS. The fuel economy improvements of using the EHPS system are therefore calculated to 3.9%.

Although the extra cost may seem prohibitive when the overall fuel savings calculated at 3.9% are taken into account this substantially offsets the extra outlay needed to install an EHPS system over the service life of the vehicle which is 500k miles.

7. Conclusion

The HyRes EHPS project aimed to demonstrate the viability and potential benefits of using an EHPS system on a hybrid electric truck. Although EHPS systems have been used in cars for many years adapting these systems for trucks has presented many new challenges.

The EHPS system that has been designed to operate at a constant speed of 1800 r/min that equates to a flow rate of 12 l/min. The power consumption of the EHPS varies with steering pressure that depends on the drive cycle of the vehicle. It was therefore necessary to analyse a representative drive cycle for the truck in order to ascertain the energy consumption in order to compare against the current HPS system.

The Farington test route provided data which was used as the baseline for the EHPS design. The route was developed in conjunction with a key truck customer to make the drive cycle as realistic as possible. What can be seen for the Farington test route is the EHPS system is more efficient compared to a conventional HPS system. At lower engine speeds there is little difference in efficiency between both systems, mainly due to the inherent electrical losses of the inverter and motor in the EHPS system.

With increasing HPS pump speeds the efficiency decreases dramatically. In comparison the efficiency of the EHPS remains relatively constant and mostly load dependent. This is because the EHPS has been optimised for the load operating at a fixed pump speed. For the Farington test route, the EHPS is significantly more efficient than the HPS system. It must be borne in mind that a different driving cycle may result in a different result favouring either system. For example if the hybrid electric truck with HPS were to be used at motorway speeds, then the EHPS system efficiency would be much higher due to the higher engine speed of the conventional truck's engine.

An EHPS system has the potential to dramatically increase overall system efficiency, dependent on the actual driving cycle undertaken by the truck. With the advent of increased

hybridisation and hence a more robust electrical system, increased electrification of truck ancillaries are now more realistic. Despite higher initial costs and placement limitation, an EHPS system has been demonstrated to give fuel savings compared to conventional HPS systems over a vehicle's lifetime based on simulation and hardware verification.

8. References

[1] M. J. Nunney, *Light and heavy vehicle technology* 4th ed. Oxford: Butterworth-Heinemann 2006.

[2] D. J. Leeming and R. Hartley, *Heavy Vehicle Technology* 2nd ed. Cheltenham: Nelson Thornes, 1992, pp. 154 - 163.

[3] J. W. Durstine, "The Truck Steering System From Hand Wheel to Road Wheel," SAE Special Publications 730039 76P, February 1972 1973.

[4] A. W. Burton, "Control objectives and systems analysis: innovation drivers for electric power-assisted steering," in *American Control Conference, 2002. Proceedings of the 2002*, 2002, pp. 3401-3406 vol.4.

[5] F. Zoran, L. Louca, A. Stefanopoulou, J. Pukrushpan, B. Kittirungsi, and H. Peng, "Fuel Cell APU for Silent Watch and Mild Electrification of a Medium Tactical Truck," presented at the SAE World Congress & Exhibition, Detroit, MI, USA, 2004.

[6] P. E. Pfeffer, D. N. Johnston, M. Sokola, and M. Harrer, "Energy Consumption of Electro-Hydraulic Steering Systems," presented at the SAE 2005 World Congress & Exhibition, Session: Steering and Suspension Technology Symposium (Part 1 & 2 of 4): Steering, Detroit, MI, USA, 2005.

[7] P. D. Schmitt, "Prediction of Static Steering Torque During Brakes-Applied Parking Maneuvers," in *International Truck & Bus Meeting & Exhibition*, Ft. Worth, TX, USA, 2003.

[8] W. Leonhard, *Control of electrical drives*, 3rd ed. ed. Berlin ; London: Springer, 2001.

[9] K. Zhou, J. C. Doyle, and K. Glover, *Robust and optimal control*. Upper Saddle River, N.J.: Prentice Hall ; London : Prentice-Hall International, 1996.

[10] G. E. Franklin, J. D. Powell, and A. Emami-Naeini, *Feedback Control of Dynamic Systems*, 3rd ed.: Addison-Wesley Publishing Company, 1994.

[11] K. J. Åström and T. Hägglund, *PID controllers*, 2nd ed. Research Triangle Park, N.C.: International Society for Measurement and Control, 1995.

[12] J. Henderson, "Steering component costs," ed. Leyland: Leyland Trucks, 2010.

[13] "Department of Energy, "Electric and Hybrid Vehicle Research," in *Development, and Demonstration Program; Petroleum-Equivalent Fuel Economy Calculation* vol. 36986, ed: DOE, 2000.

[14] P. Weissler. (2009) Many factors figure in fuel-economy calculation for electric vehicles. *Automotive Engineering International*. Available: http://www.sae.org/mags/aei/6559/